International Scholars Journals

African Journal of Geography and Regional Planning ISSN 3627-8945 Vol. 7 (3), pp. 001-014, March, 2020. Available online at www.internationalscholarsjournals.org © International Scholars Journals

Full Length Research Paper

Fuzzy logic and neural network approaches for land cover mapping of the Brazilian territory

Fernanda de Almeida Prado[1]*, Maria de Lourdes Bueno Trindade Galo[1] and Edson Eyji Sano[2]

[1]Universidade Estadual Paulista, Faculdade de Ciências e Tecnologia, Rua Roberto Simonsen n. 305, 19060-900, Presidente Prudente - SP, Brasil.

[2]Empresa Brasileira de Pesquisa Agropecuária, BR-020 km 18, Planaltina, 73301-970, Caixa Postal 08223, Brasília - DF, Brasil.

Accepted 14 November, 2019

Land cover mapping is important for regional and urban plannings. Most of the digital remote sensing based mappings use conventional classification techniques which are limited in their ability to define a wide variety of the existing types of land cover. The objective of this paper is to analyze the potential of fuzzy logic and artificial neural network approaches to produce land cover maps of the Brazilian territory for regional scales and urban environments. Two case studies were developed to test the methodological approach. Reliability analysis of resulting thematic maps was conducted through statistical coefficients and uncertainty measurements. Results showed that the use of fuzzy logic and artificial neural network approaches are suitable to fulfill the land cover mapping needs of the Brazilian territory.

Key words: Land cover mapping, fuzzy classification, artificial neural network, hierarchical classification.

INTRODUCTION

Currently, there are a number of regional land use and land cover (LULC) classification systems in the literature. They vary in structure, type and legend. Some are hierarchical, with at least two levels. They can also be broad or site-specific and focused on a particular LULC group. Classification systems with a wide variety of classes and with clear descriptions of their meanings can be considered as optimal. Two major hierarchical land cover classification systems were proposed by Anderson et al. (1976) and by the CORINE Land Cover Program (EEA, 1995). The first system includes two levels and is an open system, allowing further developments of more detailed and appropriate classifications. CORINE was developed to attend the European need for a continental and environmentally oriented dataset that would enable smooth and periodic updates. It presents three levels of detail.

In Brazil, the main references are the Technical Manual of Brazilian Vegetation (IBGE, 1992) and the Land Use Project from IBGE (2006). In the Technical Manual, the Brazilian vegetation was subdivided into four groups: Phytoecological regions, pioneer formations, vegetation refugees and areas of ecological tension (contact between two or more phytoecological regions). The Land Use Project arose from the need of a nationally adjusted standards and criteria to be used in mapping activities. The system, which is now in its second edition, was defined in three hierarchical levels and legend with maxi-mum meaning and minimum levels. The main focus of this project was the land use instead of the remaining natural vegetation.

Regarding the urban mappings, legends are usually site-specific and application-specific, resulting in a great variety of legends. Some of them are hierarchically structured, such as the one proposed by the United Nations Food and Agriculture Organization (FAO) (Di Gregorio, 2004). This author considered urban areas in the context of artificial surfaces and associated areas, defining them as impervious areas: original, natural cover replaced by artificial ones. Urban areas were divided into linear and nonlinear patterns (for instance, roads and blocks, respectively). Herold et al. (2002) also proposed a system that models urban space in three levels. The first level subdivides urban

*Corresponding author. E-mail: rado_fernanda@yahoo.com.br. Tel: +55 71 91546316. Fax: +55 71 21058601.

landscape into vegetated areas and buildings. Pinho et al. (2007) classified the city of São José dos Campos, Brazil, according to the types of materials covering the buildings. Other studies that contri-buted to the definition of legend for urban scale mappings were conducted by Silva Filho et al. (2005) and Araujo et al. (2007).

Classification systems based on remote sensing data often use visual interpretation (Araújo Filho et al., 2007) or pixel-by-pixel image classification techniques (Reys, 2008), especially for regional mappings. In these cases, results can be inconsistent, for instance, if mixed land coverages are present. Consequently, there is a demand for more complex classification techniques, such as the fuzzy approach. Conventional classifiers force pixels composed of different targets to be assigned to the most representative one (Foody, 1992). In the fuzzy logic approach, probability and uncertainty measures provided by the classifier during the mapping process are con-sidered. Urban landscapes often present different types of coverage with similar spectral signatures, so that conventional classification techniques based solely on spectral information are limited. Again, more complex processing techniques, such as the object-oriented or the artificial neural network approaches which incorporate attributes as geometry are more recommended. The objective of this paper is to analyze the potential of the fuzzy logic and artificial neural network techniques to produce land cover maps of the Brazilian territory at regional and urban scales, respectively.

MATERIALS AND METHODS

Legends

The proposed legend for regional land cover mapping of the Brazilian territory (Table 1) was based on the studies conducted by Anderson et al. (1976), EEA (1995), and IBGE (1992, 2006); EEA, 1995; IBGE, 1992, 2006). Additionally, support from the following works was also obtained: FAO (Di Gregorio, 2004); Ministry of Natural Resources of Ontario (OMNR, 1999); Project of Land Use and Land Cover of Arkansas, USA (Gorham, 1999); European Project of Land Use/Cover Area Frame Statistical Survey (LUCAS) (EC, 2006) and System of Land Use and Land Cover of Michigan, USA (MDNR, 2001). A wide variety of classes was analyzed to make necessary adjustments. The legend includes three levels and preference was given for those land cover classes more easily identified in satellite or airborne remotely sensed products.

Level I was primarily defined based on the CORINE Land Cover Project, with few modifications. Level II was based on various systems and adjustments to better fit the characteristics of the existing land cover classifications and ecosystems of Brazil. The legend proposed by IBGE (1992) for phytoecological regions was reduced to three classes (forestland, shrubland and grassland). Classes not occurring in Brazil were disregarded (e.g. tundra).

Level III was based mainly on the systems proposed by the CORINE Land Cover Project and by the Technical Manual of Brazilian Vegetation. Forestland was subdivided in dense forestland, open forestland, mixed forestland, deciduous forestland and semi-deciduous forestland. As these subclasses can occur in specific regions of the country, it is necessary to know, beforehand, the characteristics of the area to be mapped in order to choose the proper types of forests. Shrubland was subdivided according to the dominance of trees, shrubs or grasses: arboreous savanna, shrub savanna and herbaceous savanna, respectively. Grassland, which is characterized by the lack of tree species, was specified according to the dominance of shrubs or grasses: shrub grassland and herbaceous grassland.

Level I is related to global, exploratory scale (between 1:1,000,000 and 1:500,000), level II is related to regional scales (between 1:250,000 and 1:100,000) and level III is related to semi-detailed scales (larger than 1:100,000). Users can also develop their own levels IV and V to meet their specific mapping needs. Another possibility is to make slight adjustments to the proposed classes in levels II and III to better fit the specific purposes of each user, or even introduce few new classes not included in the proposed system. Detailed description of the classes found in level III category can be found in Prado (2009).

The proposed legend for urban mapping considers a large number of classes on purpose to attend different needs of mappings and several conditions of study areas. It was based mainly on the studies conducted (Herold et al., 2002; Di Gregorio, 2004; Pinho et al., 2007). The legend also consists of levels I, II and III (Table 2), encompassing 4, 10 and 27 classes, respectively. Again, more levels can be developed, depending on the need of users. The legend is self-comprehensive.

Study areas

For regional approach, the study area corresponded to the municipality of Presidente Prudente, located in the Western part of São Paulo State, Brazil, between 21°40' and 22°15' of south latitude and between 51°10' and 51°32' of west longitude. It has an extension of 562 km² and more than 200,000 inhabitants. For urban approach, the study area corresponded to a smaller portion of the Presidente Prudente city, located between 22°06' and 22°07' of south latitude and between 51°23' and 51°25' of west longitude (northern part of the city) (Figure 1).

Image processing and analysis for the regional mapping

A Landsat TM image (path/row: 222/75; overpass: September, 2007) was obtained from the National Institute for Space Research (INPE) homepage (http://www.dgi.inpe.br/CDSR/) and georeferenced to the Universal Transverse Mercator (UTM) projection system and SAD69 datum (South American Datum 1969). A set of 20 control points for geometric correction of TM image was obtained from the vector-format layers of roads, hydrography and topography, prepared and released by the Presidente Prudente´s City Hall. Linear transformation function and interpolation of brightness values by the nearest neighbor method were used for image registration. The image registration accuracy was 0.55 pixels. The image was processed using fuzzy logic approach implemented in the IDRISI™ image processing software package (Figure 2).

The interpretation key was based on the following elements of interpretation: color, shape, texture, pattern and location. Pure and mixed pixel samples of representative classes were obtained from the Landsat TM false-color composite. Mixed pixels represent the spectral signatures of regions corresponding to the gradual transition between two specific classes.

The fuzzy partition matrix, which indicates the membership degree of each set of training samples for each class, was generated in the form of a table with *n* columns, which represent the land cover classes and *m* rows, related to the training sets. The matrix considers the mixing percentages between the mapped

Table 1. Proposed legend for land cover mapping of the Brazilian territory at regional scales.

Levels		
I	**II**	**III**
Constructed surface	1.1 Urban/rural building	1.1.1 Urban/rural building
	1.2 Road/Railway	1.2.1 Road 1.2.2 Railway
Crop-livestock integrated area	2.1 Cropland	2.1.1 Permanent cropland* 2.1.2 Annual cropland* 2.1.3 Bare soil/straw
	2.2 Pastureland	2.2.1 Cultivated pastureland 2.2.2 Degraded pastureland
	2.3 Reforestation/Forestation	2.3.1 Reforestation/Forestation with *Pinus* 2.3.2 Reforestation/Forestation with *Eucalyptus* 2.3.3 Reforestation/Forestation with other species**
Wetland	3.1 Continental wetland	3.1.1 Marsh 3.1.2 Floodplain 3.1.3 Palm
	3.2 Coastal wetland	3.2.1 Salt marsh 3.2.2 Mangrove 3.2.3 Restinga 3.2.4 Saline
Water	4.1 Continental water	4.1.1 Water course 4.1.2 Lake/Pond 4.1.3 Reservoir
	4.2 Marine water	4.2.1 Bay/Estuary 4.2.2 Coastal lagoon 4.2.3 Sea/Ocean
Natural vegetation	5.1 Forestland	5.1.1 Dense forestland 5.1.2 Open forestland 5.1.3 Mixed forestland 5.1.4 Decidual forestland 5.1.5 Semi-decidual forestland
	5.2 Shrubland	5.2.1 Arboreous savanna 5.2.2 Shrub savanna 5.2.3 Herbaceous savanna
	5.3 Grassland	5.3.1 Shrub grassland 5.3.2 Herbaceous grassland
Non-vegetated area	6.1 Non-vegetated area	6.1.1 Bare soil 6.1.2 Degraded area 6.1.3 Beach/Dune/Sand

*The class name can be retained or replaced by the crop type(s) in concern. **The class name can differ depending on the species in concern.

Table 2. Proposed legend for urban land cover mappings.

Levels		
I	**II**	**III**
1 Constructed surface	1.1 Covering material	1.1.1 Ceramics 1.1.2 Asbesto-cement coverage 1.1.3 Concrete 1.1.4 Metallic coverage 1.1.5 Asphalt 1.1.6 Plastic coverage 1.1.7 Glass coverage 1.1.8 Paving stone 1.1.9 Wood coverage 1.1.10 Other cover type*
2 Vegetated area	2.1 Natural/planted vegetated area	2.1.1 Tree/Shrub 2.1.2 Grass
	2.2 Vegetated wetland	2.2.1 Vegetated wetland
	2.3 Crop-livestock integrated area	2.3.1 Bare soil/straw 2.3.2 Cropland** 2.3.3 Pastureland 2.3.4 Reforestation/Forestation***
3 Non-constructed / non-vegetated area	3.1 Bare soil	3.1.1 Sand 3.1.2 Rock 3.1.3 Soil
	3.2 Non-vegetated wetland	3.2.1 Non-vegetated wetland
	3.3 Degraded area	3.3.1 Degraded area
	3.4 Shadow	3.4.1 Shadow
4 Water	4.1 Natural water	4.1.1 Water course 4.1.2 Lake/Pond 4.1.3 Sea
	4.2 Artificial water	4.2.1 Reservoir

*The class name is defined according to the type of covering material. **The type of existing crop is used to represent the class name. ***The class name is defined depending on the considered species.

classes occurring in the training samples. Therefore, the analyst has to estimate the proportion of occurrence of each class based on the collected training data. The extraction of fuzzy signatures produces an output in which each pixel is assigned a weight proportional to its membership degree in the estimation of mean, variance and covariance of each band and thematic class of interest. For example, a pixel predominantly composed of forest will have high weight in determining the signature related to this class, but a low weight for other classes.

Bayesian soft classification was applied considering a priori equal probability for all classes. Result of processing was a set of images (one per class) that expresses a posteriori probability of the pixels belonging to each land cover class and an additional image that represents the classification uncertainty. A single classified image was generated from a posteriori probability images assigning each pixel to the class more likely to belong to that class. The Bayesian soft classification technique allows the analysis of the reliability of the mapping in two ways: From the calculation of statistical metrics indicating the mapping accuracy or from uncertainty measures associated with the decision process for the allocation of the pixels to the classes. For the first analysis, we used an error matrix that is generated by considering the following factors: reference data, type of sample unit, number of sample elements and sampling scheme (Congalton and Green, 1999).

The reference data used were: knowledge of the study area, interpretation of high spatial resolution images provided by the

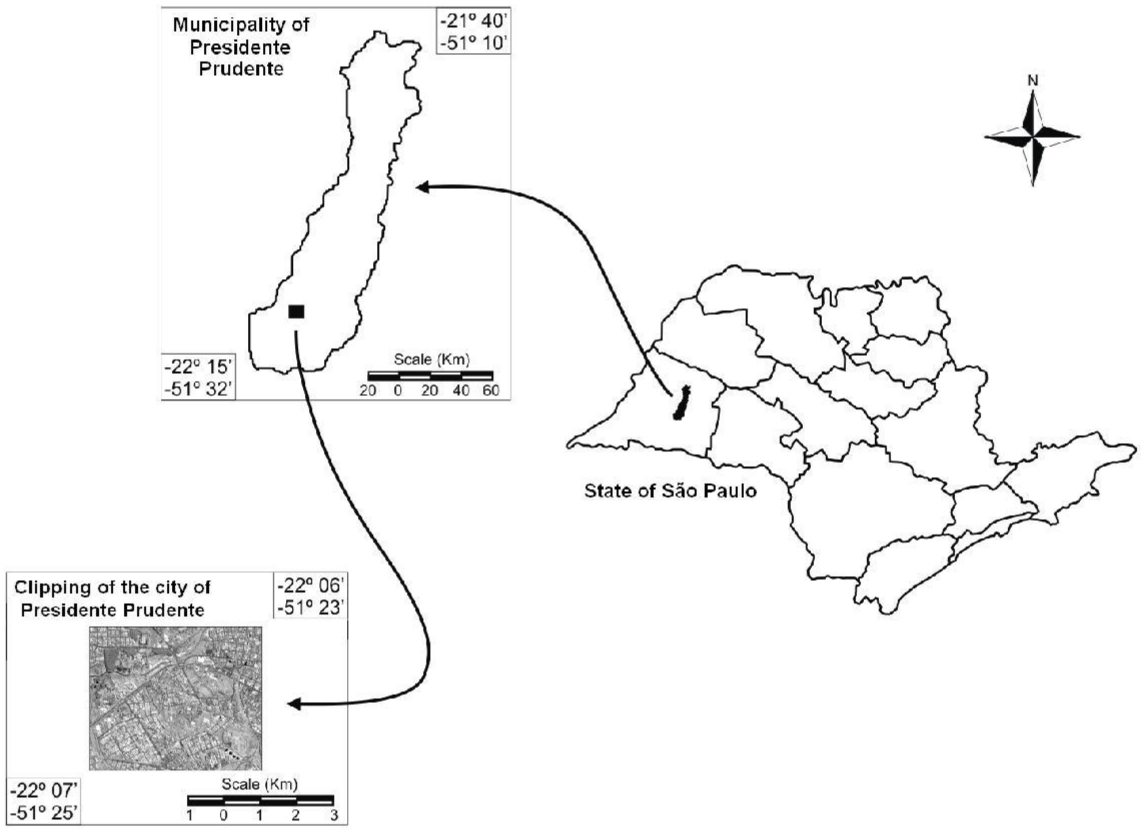

Figure 1. Location of the study areas in the State of São Paulo, Brazil.

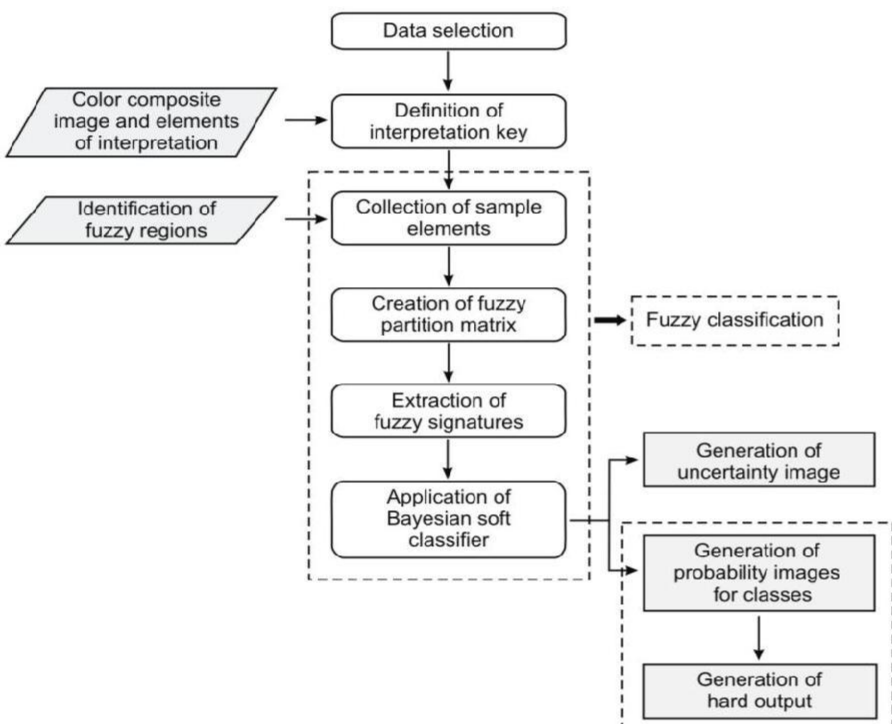

Figure 2. Flowchart for the proposed fuzzy logic approach.

Google Earth™ program and information from the CANASAT Project (http://www.dsr.inpe.br/mapdsr/) which provided the spatial distribution of areas cultivated with sugarcane in the municipality of Presidente Prudente. Regarding the sample units, we considered a cluster of 2 pixels by 2 pixels and the stratified random sampling, since it combines low potential for bias (random scheme) with greater coverage (stratification), ensuring that a minimum number of samples is selected for each stratum. The appropriate number of sampling units per class was determined by the polynomial distribution model, which implies a priori knowledge of the number of classes and their proportions in the map (Equation 1):

$$n_i = \chi^2_{(1,1-(\alpha/m))} \, p_i \left(1 - p_i\right) / d_i^2 \, ; \tag{1}$$

where n_i is the sample size for the class *i*, with *i* = 1, 2 ,…, *m*; $\chi^2_{(1,1-(\alpha/m))}$ is the value for the desired confidence level (α/m) with one degree of freedom and $(1-\alpha/m)$, considering the chi-square distribution; p_i is the representative proportion of the class *i* in the mapping and d_i is the allowable error (or desired accuracy). The minimum number of samples (n) to be considered for each class is:

$$n = \max_i \left\{ n_i / m \right\}. \tag{2}$$

The thematic accuracy was obtained (0.5 cm) from the error matrix and computed by the overall accuracy and Tau and Kappa coefficients. We also calculated the correlation coefficients for individual classes, specifically the user's accuracy (UA) and the producer's accuracy (PA), which reflect the commission and omission errors, respectively, as well as the Kappa index for each class (Congalton and Green, 1999).

As statistical coefficients are global indices, they consider entire map in the reviewing process so that the overall qualities provided by these indices are often a satisfactory standard. However,

it does not mean that quality is maintained uniformly throughout the mapping. Significant variations may exist in some areas and they might be of particular interest to some users. Then, a spatial representation of the highest uncertainty points in the classification can indicate the presence of local variations in the quality of the map. Thus, not only the mapping accuracy but also the assessment of the spatially distributed uncertainties in the map has to be addressed.

The uncertainty introduced during the remote sensing data classification can be characterized by probability vectors that are produced as a by-product of the classification and may be indicative of dubious classifications, mixed pixels, heterogeneous classes or ambiguous boundaries between classes (Goodchild et al., 2002).

The uncertainty in x_i $Inc(x_i)$ can be determined by a single probability value: the probability of the modal class (*c* = 1,…, *m*)

associated with the position x_i . Therefore, the uncertainty was estimated by:

$$Inc(x_i) = 1 - P\left(\omega_c \mid x_i\right). \tag{3}$$

where *i* = 1,…, *n* and $P(\omega_c \mid x)$ is a posteriori probability of attributes vector x_i belonging to the considered class.

Image processing and analysis for the urban mapping

Two QuickBird II satellite images with 2.44 m (multitespectral image) and 61 cm (panchromatic image) spatial resolutions were obtained (overpass: February, 2007). These images were acquired in standard correction level and were made available by Professor Dr. Amilton Amorim from the Department of Cartography of the FCT/UNESP, through research project funded by the São Paulo Research Foundation (FAPESP).

The images were georeferenced to the UTM projection system and SAD69 datum considering a linear transformation and interpolation by the nearest neighborhood. A set of 20 control points identified in the vector database were used to georeference the panchromatic image, achieving an accuracy of 3.14 pixels. Taking the corrected panchromatic image as a reference, another 20 control points were used to register the multispectral image, resulting in an error of 0.42 pixels.

Panchromatic and multispectral images were then merged using the Gram-Schmidt technique (Laben and Brower, 2000). Then, it was generated an occurrence texture image using an entropy filter with window size of 9 pixels by 9 pixels. This procedure allows the combination of spatial and spectral information in the classification process, minimizing the spectral similarity of some targets. Preliminary tests conducted with conventional classifiers indicated, for example, confusion between asphalt and asbesto-cement and between soil and red ceramics.

The four fused Quickbird bands and texture image were used to perform an artificial neural network (ANN) classification. The steps required for the thematic information extraction are illustrated in Figure 3.

Training and validation samples were obtained for each land cover class. The architecture specified was a multilayer feedforward network, which requires the definition of an input layer, one or more hidden layers and output layer. Simulations were carried out with one or two hidden layers. The performance of the trained network was verified with backpropagation learning algorithm. The number of nodes in the input layer was defined by the size of input data, that is, the four fused bands and the texture image with five nodes.

The supervised training process using backpropagation involves a prior selection of all samples and indication of the number of training and validation pixels to be considered for each class. Furthermore, it was necessary to define in advance the training parameters, which includes the learning rate, the momentum factor and the stopping criterium. The last one controls the end of the process and includes three aspects: the value of the acceptable mean square error (MSE), the number of iterations and the accuracy rate. Several simulations were performed varying the number of iterations and analyzing the training statistics, which included: values of the test and validation errors, number of iterations and accuracy rate computed from the test and validation pixels collected for the classes.

After training the ANN, the classification was performed generating conventional (hard) and soft outputs of the thematic classes, which express the membership degrees (activation levels) of the pixels in relation to each class. In order to minimize the number of isolated pixels within the classified regions and pixels located in the edge regions (transition between classes), where a large amount of misclassified pixels can occur, the mode filter was applied on the classified image, considering a 5 × 5 window and setting the final classification result.

To assess the reliability of the urban scale mapping, statistical indices (overall and by class) and their corresponding uncertainty measurements were calculated. The reference data were based on three-day field survey. The random sample unit was a cluster of 3 pixels by 3 pixels. The number of sample elements per class was calculated using Equations 1 and 2. The analysis of mapping uncertainty was based on the soft images that express the activation levels of output for each pixel for each class, which are a

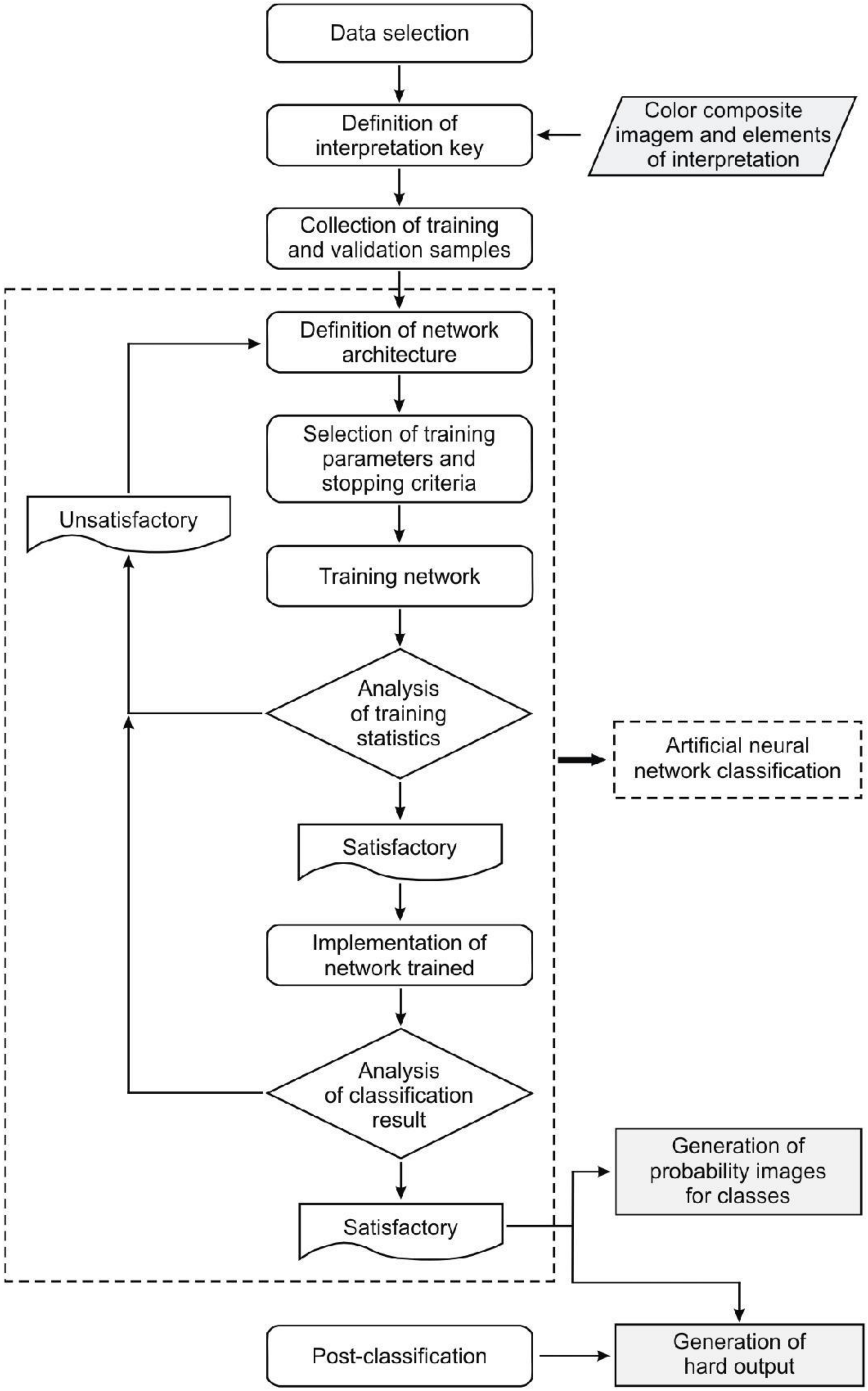

Figure 3. Flowchart for the artificial neural network classification.

Table 3. Fuzzy partition matrix.

m	n							
	URB	**RR**	**CP**	**PT**	**CWE**	**CWA**	**FL**	**NVA**
1	0.85	0.10	0	0	0	0	0	0.05
2	0	1	0	0	0	0	0	0
3	0	0	1	0	0	0	0	0
4	0	0	0	0.86	0.06	0	0.08	0
5	0	0	0	0	0.80	0.14	0.06	0
6	0	0	0	0	0	1	0	0
7	0	0	0	0	0	0	1	0
8	0	0	0	0	0	0	0	1

URB = Urban/rural building; RR = road/railway; CP = cropland; PT = pastureland; CWE = continental wetland; CWA = continental water; FL = forestland; and NVA = non-vegetated area.

product of the ANN classification.

RESULTS

Regional mapping

Among the 13 classes listed in the level II of the proposed system (Table 1), we identified the following classes in the municipality of Presidente Prudente:

1. Urban/Rural building: urban spots of the city of Presidente Prudente and districts;
2. Road/Railway: street and highway network in the city;
3. Cropland: annual and permanent crop area, including bare soil prepared for plantation and straws derived from freshly harvested crop;
4. Pastureland: cultivated pastures used by cattle raising;
5. Continental wetland: wetland surrounding water courses;
6. Continental water: natural and artificial water courses and water bodies;
7. Forestland: remaining semi-deciduous, seasonal forest;
8. Non-vegetated area: region with outcrops and degraded area formed by the city´s landfill.

From the training samples collected for each thematic class, we defined the fuzzy partition matrix (Table 3). For all samples collected for urban/rural building, for example, it was estimated a proportion of 85% of occurrence of the class itself, 10% of occurrence of road/railway and 5% of non-vegetated area. This estimate was based on the training data collected for each class and the membership degrees that have been assigned considering the knowledge of the analyst in the image interpretation. When there was no mixing ratio in the set of training samples, the value 1 was assigned to the class (e.g. continental water).

In Figure 4, we presented two examples of a posteriori probability images (result of the Bayesian soft classification) of the municipality of Presidente Prudente for urban/rural building (A) and pastureland (B). The color scale shows that the northeastern part of the municipality has low probability to be either constructed area or pastureland, since both images A and B provided a low posteriori probability for the pixels on this site. These pixels may belong to any other mapped class, consequently, their probability images should be analyzed to identify the classes in which the pixels are more likely to belong to them (class). In image A, there is a high a posteriori probability of the pixels to represent mainly an urban area located in the southwestern part of the municipality. In image B, we can notice a large portion of the municipality with high a posteriori probability of belonging to pastureland, which means that, in the remaining probability images, the pixels located in these regions have lower probabilities of belonging to this class.

By forcing the pixels to be assigned to the classes that have higher probability of belonging to them, one can obtain a hard output of the soft classification, which corre-sponds to the land cover map of the municipality of Presidente Prudente (Figure 5).

Based on the random distribution of 278 sampling units in the images, we obtained the following overall accuracy, Tau and Kappa indices: 85.63, 83.58 and 81.67%, respectively. As expected, the overall accuracy presented the highest percentage, since it considers only the correct percentage of the matrix. Tau and Kappa coefficients consider both the percentage of full agreement and the proportion of agreement by chance. The intermediate value of Tau indicates a balance between the other two indices.

For the accuracy assessment per class, the estimated values for UA, PA and Kappa index per class ($\hat{\kappa}_i$) are listed in Table 4. Continental water showed the highest UA, that is, no pixel was misclassified in this class. This is one of the targets more readily extracted in the images,

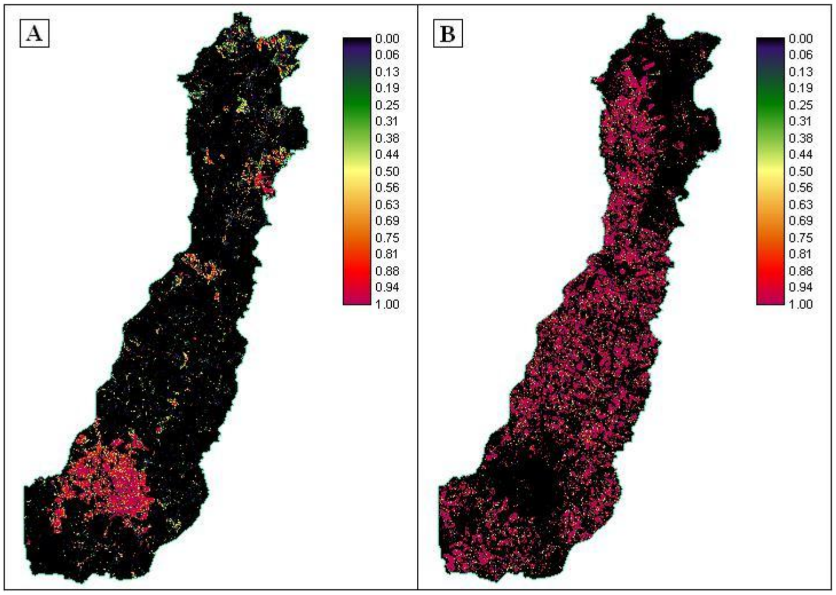

Figure 4. A posteriori probability images for (A) urban/rural building and (B) pastureland.

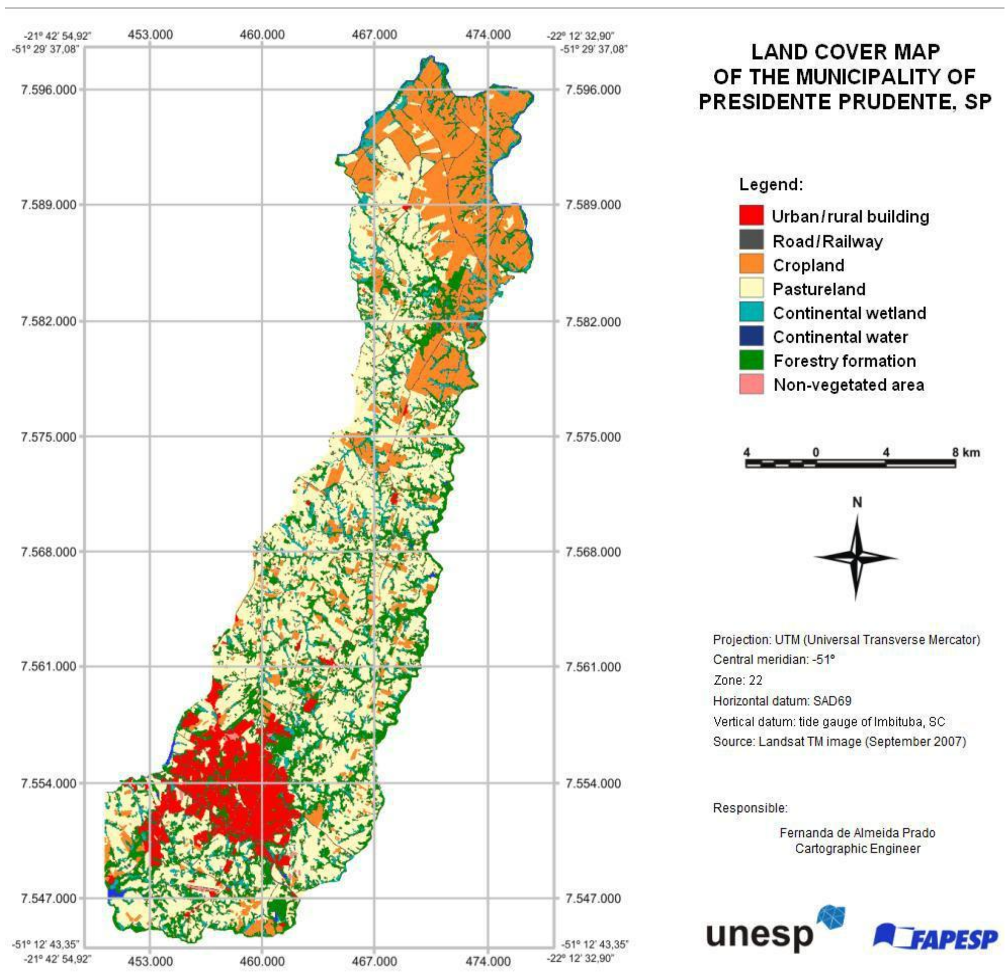

Figure 5. Land cover map of the municipality of Presidente Prudente, SP.

Table 4. Accuracy indices per class computed in the regional scale mapping.

Land cover class	UA (%)	PA (%)	$\hat{\kappa}_i$ (%)
Urban/Rural building	80.13	85.03	77.29
Cropland	88.72	82.01	85.22
Pastureland	84.21	89.64	77.33
Continental wetland	82.61	73.64	80.47
Continental water	100.00	78.26	100.00
Forestland	88.98	93.33	86.38
Non-vegetated area	78.57	64.71	78.26

UA = User's accuracy; PA = producer's accuracy; $\hat{\kappa}_i$ = Kappa agreement index.

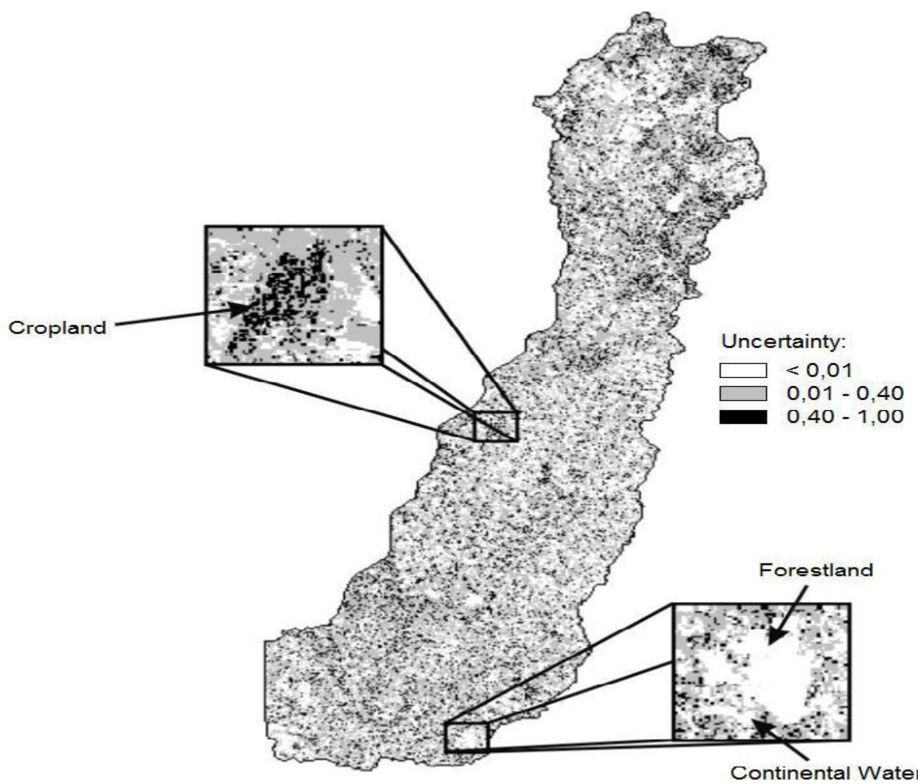

Figure 6. Uncertainty image generated by the Bayesian soft classifier.

mainly from images obtained in the near and middle infrared spectral range, where electromagnetic energy is strongly absorbed by water bodies. Non-vegetated area provided the lowest rate of UA, because this class presented spectral patterns similar to urban/rural building and cropland.

The highest rates of PA were computed for pastureland, the most extensive land cover class in the study area and forestland, which is easily discriminated in the satellite images, especially when they are obtained in the red and near infrared spectral ranges. Non-vegetated area resulted in the lowest rate of PA. Kappa indices per class were close to those calculated for the UA since both statistics are computed considering the marginal totals of the error matrix provided by the classification result. Although the results were similar, Rosenfield and Fitzpatrick-Lins (1986) recommended the consideration of the Kappa index.

The spatial analysis of the uncertainty is as shown in Figure 6, which indicates the regions with higher and lower probability error in the allocation of pixels to the classes. A dominance of gray tone was observed in most of the study area, indicating an uncertainty ranging from 1 to 40%. Some regions showed rather low uncertainties, such as the continental water and forestland classes.

Conversely, other regions showed high uncertainty.

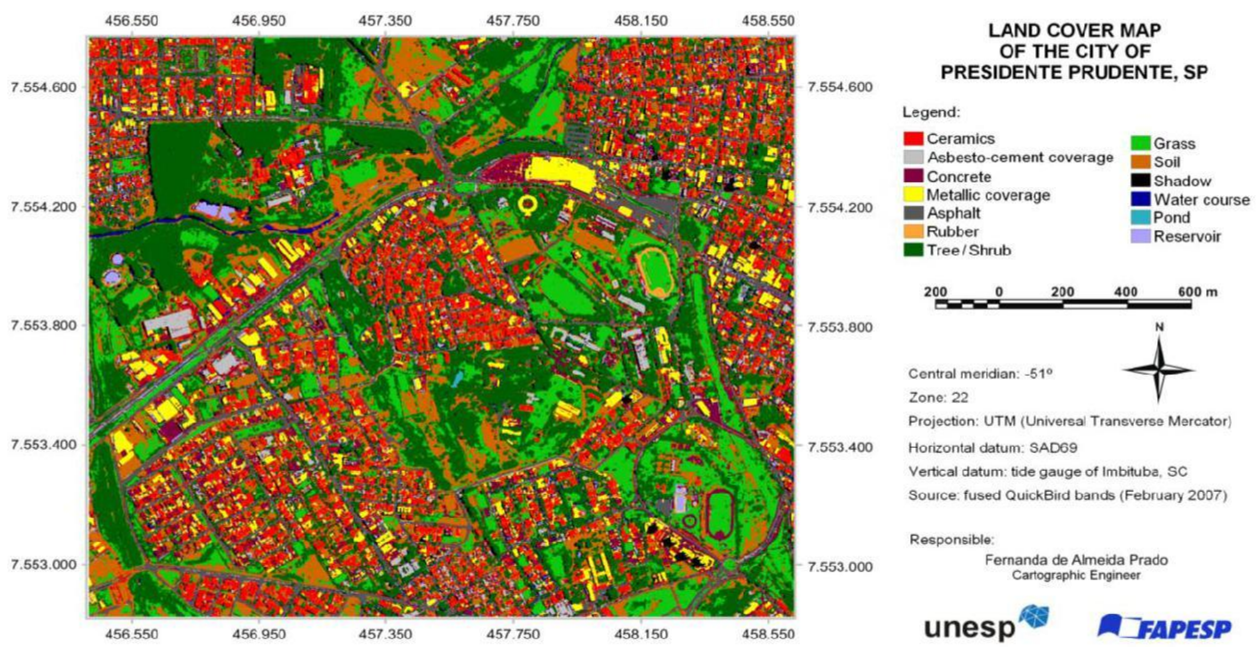

Figure 7. Urban land cover map of the part of the city of Presidente Prudente, SP.

This was the case of cropland, which presented spectral confusion with non-vegetated area and mainly urban/rural building.

Urban mapping

We identified 13 classes, from a total of 27 classes at the level III detailing:

1. Ceramics: building coverage or pavement made of different colored pottery;
2. Asbesto-cement coverage: building coating consisting of asbesto-cement;
3. Concrete: building coverage consisting of concrete (exposed slab), concrete pavements and sports courts;
4. Metallic coverage: building coating made of metallic material consisting of aluminum, steel or copper;
5. Asphalt: asphalt coating used in most roads and railways;
6. Rubber: synthetic rubber coating used on athletics tracks;
7. Tree/Shrub: vegetated area with clusters of trees or isolated trees and shrubs;
8. Grass: vegetated area consisting of grass cover;
9. Soil: exposed area composed of sand, rock or soil;
10. Shadow: shade area surrounding trees and buildings;
11. Water course: natural, linear fresh water body formed by Córrego do Veado, that is, one of the main water courses found in the city of Presidente Prudente;
12. Pond: natural, fresh water body;
13. Reservoir: artificial water body intended for water and effluents treatments and for leisure.

The output layer provided by the ANN consisted of 13 nodes (0.5 cm), that is, 13 land cover classes. Furthermore, we selected two hidden layers with 25 and 18 nodes in the first and second layers, respectively, since the use of a single layer was insufficient to handle such a variety of classes. Regarding the learning rate that normally corresponds to the proportion of error that is passed onto the nodes during the iterations, the best-fit value was 0.001. The momentum factor, which controls the convergence speed of the network, was defined as 0.5.

Final accuracy and squared mean error results obtained after the network training corresponded to 85.97% and 0.00045, respectively. These results were achieved considering the architecture of 5-25-18-13, learning rate of 0.001, momentum factor of 0.5 and 7,000 iterations. Result of ANN classifier for the study area is as shown in Figure 7.

Considering 197 samples, we estimated the overall accuracy, and Tau and Kappa agreement indices: 84.66, 83.38 and 82.47%, respectively. The values of UA, PA and the Kappa index per class ($\hat{\kappa}_i$) are listed in Table 5.

Rubber, tree/shrub and pond showed 100% of UA. Rubber and pond were the classes with lowest area extent in the study area. Tree/Shrub was also easily discriminated from the fused band 4. Concrete provided the lowest rate of UA due to spectral similarity with other targets. The highest rates of PA were obtained again for rubber and pond, as well as for grass, due to the incorporation of band 4 in the classification process.

Ceramics resulted in the lowest PA, caused mainly by the spectral confusion with concrete and soil. From the

Table 5. Accuracy indices per class computed for the urban scale mapping.

Land cover class	UA (%)	PA (%)	$\hat{\kappa}_i$ (%)
Ceramics	72.86	71.78	69.38
Asbesto-cement coverage	78.57	74.32	77.64
Concrete	64.67	79.87	61.43
Metallic coverage	78.50	96.55	77.40
Asphalt	80.14	84.17	78.45
Rubber	100.00	100.00	100.00
Tree/Shrub	100.00	87.38	100.00
Grass	85.65	100,00	83.86
Soil	95.40	77.09	94.38
Shadow	75.00	85.71	74.08
Water course	69.44	96.15	68.52
Pond	100.00	100.00	100.00
Reservoir	98.15	92.98	98.09

UA = user's accuracy; PA = producer's accuracy; $\hat{\kappa}_i$ = Kappa agreement index.

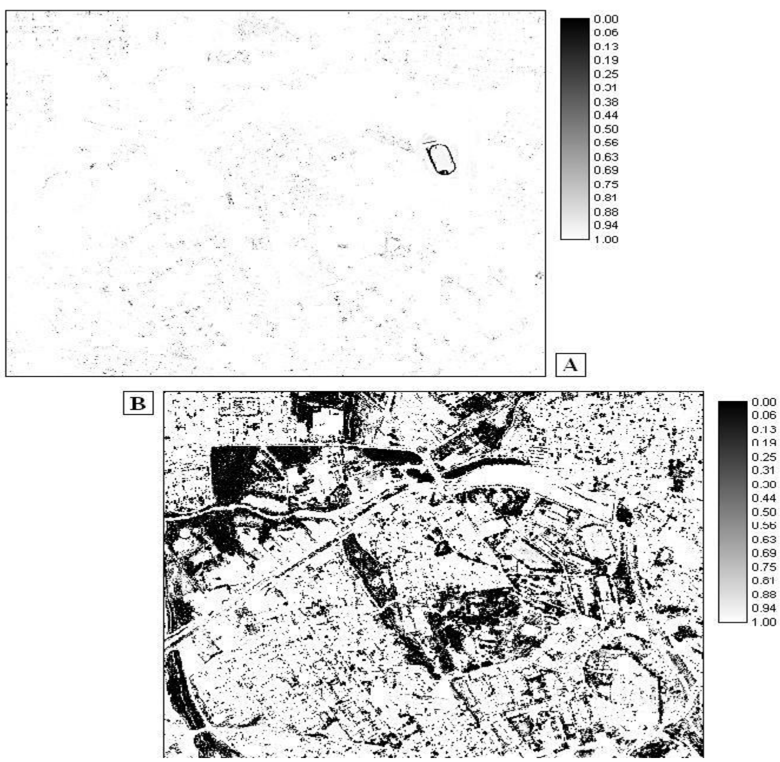

Figure 8. Uncertainty images for (A) rubber and (B) tree/shrub, generated by the artificial neural network classifier.

analysis of the by-class Kappa index, whose values are close to those obtained for the UA, the worst result was obtained for concrete, followed by water course and ceramics.

The ANN classification for urban scale mapping provided good accuracy results, particularly in the discrimination of ceramics, soil, asbesto-cement coverage and asphalt, which previously presented great difficulty of discrimination by conventional classifiers.

Regarding the mapping uncertainty, Figure 8 shows the uncertainty images for rubber (A) and tree/shrub (B). In image A, there was high membership degree for pixels

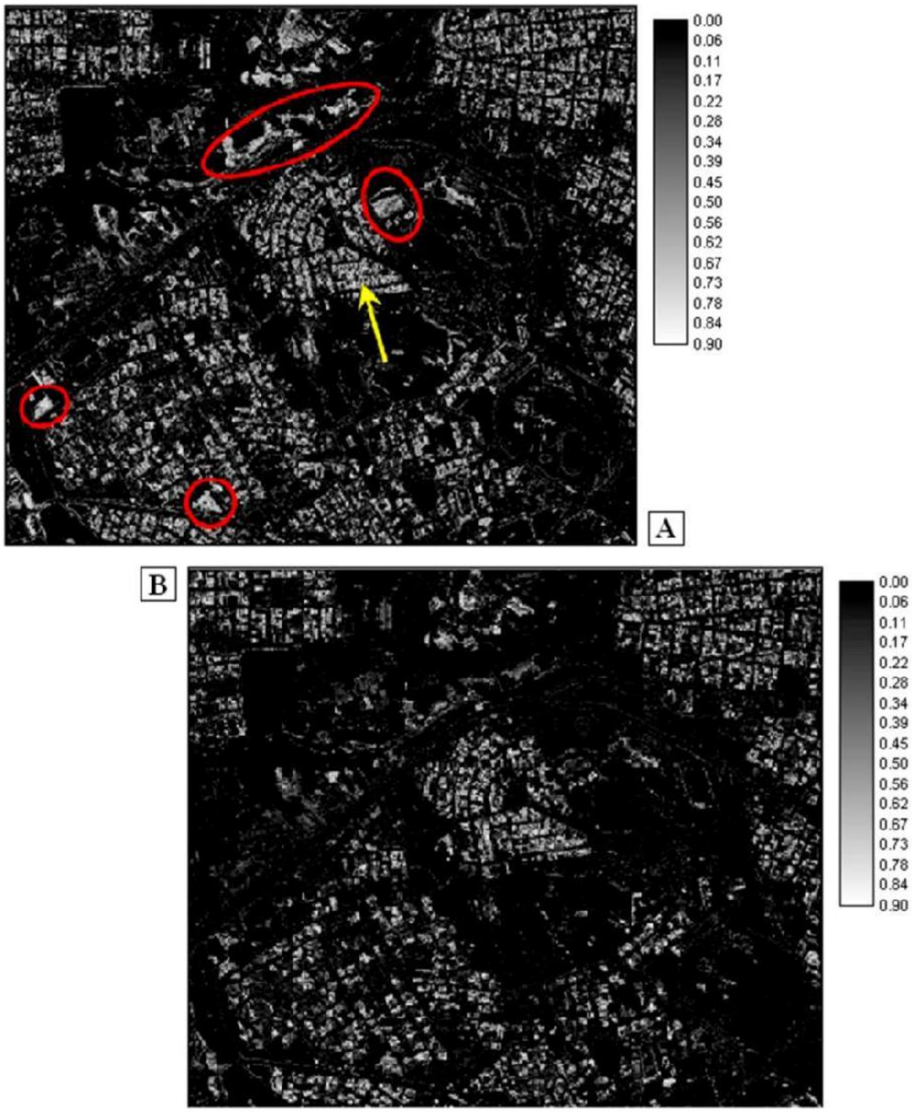

Figure 9. Outputs related to class ceramics, (A) without and (B) with the texture information.

corresponding to the rubber coating used on the athletics track, which is the only region of the study area covered by this cover type. In image B, we observed high memberships for tree/shrub in most of the study area.

One way to see the relevance of image texture in the classification process is to observe the soft outputs. For example, when ceramics is considered, which tends to be confused with soil in a classification process based solely on spectral information, the pixels belonging to both classes have similar membership degrees, causing uncertainty in decision making. This was verified by applying the ANN with only merged bands, that is, without the texture information. Figure 9A and B show the soft images generated by the classifier when tested without and with the texture information, respectively. The circled areas in the image A correspond to the soil and arrow indicates buildings covered mostly with ceramics. Both areas (soil and ceramics) presented close membership (image A) that are differentiated only when the entropy measurements assist the classifier (image B).

Conclusions

The use of fuzzy logic and ANN approaches considering two case studies revealed that they have potentials to fulfill the land cover mappings needs for the Brazilian territory. Fuzzy logic was shown to be appropriate in handling mixed satellite pixels at moderate spatial resolutions. This approach also allowed analysis of the uncertainties related to the mapping processes. In the context of urban scale mapping, ANN classification represented a good alternative to deal with information extraction from images with spatial resolutions higher than one meter.

ACKNOWLEDGEMENTS

The authors thank the UNESP´s Graduate Program in Cartographic Sciences, where this work was developed, and the São Paulo Research Foundation (FAPESP) for financial support. The National Research Council (CNPq) provided individual research grant for the third author.

REFERENCES

Anderson JR, Hardy EE, Roach JT, Witmer RE (1976). A land use and land cover classification system for use with remote sensor data. United States Geological Survey, Washington, Geological Survey Professional, Paper 964.

Araújo EHG, Kux HJH, Florenzano TG (2007). Análise multitemporal de dois bairros de Belo Horizonte (MG) usando classificação orientada a objetos de imagens QuickBird e inferências espaciais. In: Blaschke T, Kux, H (eds). Sensoriamento remoto e SIG avançados, 2nd ed., Oficina de Textos, São Paulo, pp, 209-226.

Araújo Filho MC, Meneses PR, Sano EE (2007). Sistema de classificação de uso e cobertura da terra com base na análise de imagens de satélite. Revista Brasileira de Cartografia, 59(2): 171-179.

Congalton RG, Green K (1999). Assessing the accuracy of remotely sensed data: principles and practices, Lewis Publishers, New York. Di Gregorio A (2004). Land cover classification system (LCCS), version 2: classification concepts and user manual. Food and Agriculture Organization of the United Nations, Rome.

EC – European Commission (2006). LUCAS 2006 (Land use/cover area frame survey), Technical reference document C-3: Nomenclature. Available: http://circa.europa.eu/irc/dsis/landstat/info/data/survey_documentation.htm. Access: February 6th, 2010.

EEA – European Environmental Agency (1995). CORINE land cover – part 1: methodology. EEA, Available: http://reports.eea.eu.int. Access: January 13th, 2010.

Foody GM (1992). A fuzzy sets approach to the representation of vegetation continua from remotely sensed data: an example from lowland heath. Photogramm. Eng. Remote Sensing, 58(2): 221-225.

Goodchild MF, Shi W, Fisher PF (2002). Spatial data quality, Taylor & Francis, London.

Gorham B (1999). Final report: the 1999 Arkansas land-use / land-cover project.Available:http://www.cast.uark.edu/local/arlulc99/final_report.htm.Access: February 7th, 2010.

Herold M, Gardner M, Hadley B, Roberts D (2002). The spectral dimension in urban land cover mapping from high resolution optical remote sensing. In: Jürgens C (ed), 3rd International Symposium on Remote Sensing of Urban Areas, Istanbul, Turkey, 11-13 June, pp. 77-84.

IBGE – Instituto Brasileiro de Geografia e Estatística (1992). Manual técnico da vegetação brasileira. IBGE, Rio de Janeiro, Manuais Técnicos em Geociências, n. 1.

IBGE – Instituto Brasileiro de Geografia e Estatística (2006). Manual técnico de uso da terra. 2nd ed. IBGE, Rio de Janeiro, Manuais Técnicos em Geociências, n. 7.

Laben CA, Brower VB (2000). Process for enhancing the spatial resolution of multispectral imagery using pan-sharpening. United States Patent 6011875. Available: http://www.freepatentsonline.com/6011875.html. Access: November 15th, 2009.

MDNR – Michigan Department of Natural Resources (2001). Michigan land cover/use classification system – 2000. Available : http ://www.rsgis.msu.edu/pdf/lclu/Michigan_LC_LU_Classification_System_2000.pdf. Access: March 11th, 2010.

OMNR - Ontario Ministry of Natural Resources (1999). Ontario land cover data base: user's manual. OMNR, Canada.

Pinho CMD, Kux HJH, Almeida CM (2007). Influência de diferentes padrões de ocupação do solo urbano na qualidade de mapeamentos de cobertura do solo em imagens de alta resolução espacial: estudo de caso São José dos Campos (SP). In: Blaschke T, Kux H (eds). Sensoriamento remoto e SIG avançados, 2nd ed. Oficina de Textos, São Paulo, pp 198-208.

Prado FA (2009). Sistema hierárquico de classificação para mapeamento da cobertura da terra nas escalas regional e urbana. M.S. thesis, Ciências Cartográficas, Faculdade de Ciências e Tecnologia, Universidade Estadual Paulista, Presidente Prudente, Brasil, pp. 168.

Reys S (2008). Analyzing land use/land cover changes using remote sensing and GIS in Rize, north-east Turkey. Sensors, 8: 6188-6202.

Rosenfield GH, Fitzpatrick-Lins K (1986). A coefficient of agreement as a measure of thematic classification accuracy. Photogramm. Eng. Remote Sensing, 52(2): 223-227.

Silva Filho DF, Pivetta KFL, Couto HTZ, Polizel JL (2005). Indicadores de floresta urbana a partir de imagens aéreas multiespectrais de alta resolução. Scientia Forestalis, 67(67): 88-100.